Epigenetics

ISSN: 1559-2294 (Print) 1559-2308 (Online) Journal homepage: https://www.tandfonline.com/loi/kepi20

Epigenetic alterations in folate transport genes in placental tissue from fetuses with neural tube defects and in leukocytes from subjects with hyperhomocysteinemia

Sanja A. Farkas, Anna K. Böttiger, Helena S. Isaksson, Richard H. Finnell, Aiguo Ren, Torbjörn K. Nilsson & Torbjörn K. Nilsson

To cite this article: Sanja A. Farkas, Anna K. Böttiger, Helena S. Isaksson, Richard H. Finnell, Aiguo Ren, Torbjörn K. Nilsson & Torbjörn K. Nilsson (2013) Epigenetic alterations in folate transport genes in placental tissue from fetuses with neural tube defects and in leukocytes from subjects with hyperhomocysteinemia, Epigenetics, 8:3, 303-316, DOI: 10.4161/epi.23988

To link to this article: https://doi.org/10.4161/epi.23988

Copyright © 2013 Landes Bioscience

Published online: 15 Feb 2013.

Submit your article to this journal

Article views: 719

View related articles

Citing articles: 8 View citing articles

Full Terms & Conditions of access and use can be found at
https://www.tandfonline.com/action/journalInformation?journalCode=kepi20

RESEARCH PAPER

Epigenetics 8:3, 303–316; March 2013; © 2013 Landes Bioscience

Epigenetic alterations in folate transport genes in placental tissue from fetuses with neural tube defects and in leukocytes from subjects with hyperhomocysteinemia

Sanja A. Farkas,[1,*] Anna K. Böttiger,[1] Helena S. Isaksson,[1,2] Richard H. Finnell,[3] Aiguo Ren[4] and Torbjörn K. Nilsson[1,2]

[1]Department of Laboratory Medicine; Örebro University Hospital; Örebro, Sweden; [2]School of Health and Medical Sciences; Örebro University; Örebro, Sweden; [3]Department of Nutritional Sciences; Dell Pediatric Research Institute; University of Texas; Austin, TX USA; [4]Institute of Reproductive and Child Health and Ministry of Health Key Laboratory of Reproductive Health; Peking University Health Science Center; Beijing, P.R. China

Keywords: *FOLR1*, *PCFT*, *RFC1* 80G > A, homocysteine, tissue-specific DNA methylation, GpG island, NTD

Abbreviations: *FOLR1,* folate receptor alpha; *PCFT*, proton-coupled folate transporter; *RFC1*, reduced folate carrier 1; tHcy, total plasma homocysteine; CGI, CpG island; T-DMR, tissue-specific differentially methylated region; NTD, neural tube defect; SAM, S-adenosylmethionine

The objectives of this study were to identify tissue-specific differentially methylated regions (T-DMR's) in the folate transport genes in placental tissue compared with leukocytes, and from placental tissues obtained from normal infants or with neural tube defects (NTDs). Using pyrosequencing, we developed methylation assays for the CpG islands (CGIs) and the CGI shore regions of the folate receptor α (*FOLR1*), proton-coupled folate transporter (*PCFT*) and reduced folate carrier 1 (*RFC1*) genes. The T-DMRs differed in location for each gene and the difference in methylation ranged between 2 and 54%. A higher T-DMR methylated fraction was associated with a lower mRNA level of the *FOLR1* and *RFC1* genes. Methylation fractions differed according to *RFC1* 80G > A genotype in the NTD cases and in leukocytes from subjects with high total plasma homocysteine (tHcy). There were no differences in methylated fraction of folate transporter genes between NTD cases and controls. We suggest that T-DMRs participate in the regulation of expression of the *FOLR1* and *RFC1* genes, that the *RFC1* 80G > A polymorphism exerts a gene-nutrition interaction on DNA methylation in the *RFC1* gene, and that this interaction appears to be most prominent in NTD-affected births and in subjects with high tHcy concentrations.

Introduction

Cellular intake of folate is crucial for nucleotide synthesis, methylation reactions and production of glycine and serine.[1-3] Methylation reactions of DNA, protein and RNA by S-adenosylmethionine (SAM) are normally followed further downstream by the re-methylation of homocysteine (Hcy) to methionine.[3] The cell regulates the level of Hcy primarily by excretion via the transsulfuration pathway (homocysteine is converted to cysteine), or by re-methylation.[1] An elevated plasma Hcy concentration often results from an insufficient intracellular folate or vitamin B12 supply, impeding the re-methylation of Hcy, and is therefore a convenient biomarker to identify subjects with a functional folate deficiency.[4]

In human cells, folate transport is facilitated by three types of receptors/transporters: folate receptor α (*FOLR1*), proton coupled transporter (*PCFT*) and reduced folate carrier (*RFC1*).[5] The placenta is an organ that mediates uptake of folates to the developing embryo, which are critically important for providing the nutrients needed for cellular proliferation and the development of critical structures, such as the embryonic neural tube.[6] In both humans and mice, the placenta expresses all three types of receptors.[7] Mice lacking the folate binding protein, ortholog to the human folate receptor (*hFR*α), develop structural malformations including craniofacial, cardiac and NTDs.[8-12] Inhibition of folic acid binding to FRα has been suggested as a risk factor for NTDs.[13]

DNA methylation is involved in regulating gene expression.[14] Most intervention studies of folate intake and DNA methylation are addressing global DNA methylation in blood leukocytes. Findings from the seven previously published folate intervention studies summarized by Terry and colleagues are notable for their inconsistent findings.[15] Only 2 of 7 studies found any significant changes in leukocyte global DNA methylation. These

*Correspondence to: Sanja A. Farkas; Email: sanja.farkas@orebroll.se
Submitted: 01/10/13; Revised: 02/08/13; Accepted: 02/12/13
http://dx.doi.org/10.4161/epi.23988

Table 1. PCR primers forward (F), reverse (R) and sequencing primers (S) used for the *FOLR1* gene pyrosequencing methylation assays

CpG site no.	Nucleotide no.*	Primer sequence, 5'-3'	T_a (°C)	Size (bp)
1 & 2	116, 146	F: GGG TTA GGA TTG AGT TTT TTA ATG TTT G	59	93
5'CGI shore		R: biotin- AAC CCA CCT ACT CAT ACA ACT T		
		S: TGA GTT TTT TAA TGT TTG TAT GAA		
3–5	712, 716, 748	F:GTT TTT TTA AAG TGT GGG ATT ATA GAA ATG	57.5	93
5'CGI shore		R: biotin-AAA AAC ACA ACC CAA AAT TTT AC		
		S: GTG GGA TTA TAG AAA TGA G		
6–8	2508, 2518, 2524	F:GGT TAG GAT GGT TTT GAT TTT TTA GTT	52.9	263
CGI		R: biotin-ACC CCA AAC TAA ATA CAA TAA CTT ACT T		
		S: AAA ATG TTG GGA TTA TAG G		
9–11	3457, 3466, 3477	F: GTT GGG ATT TTT GAA TTT GAG TTT	61	125
3'CGI shore		R: biotin-TCT TCC CAC CAT TAC TCA CAA		
		S: TGT ATT AAA ATT ATT TAG GTG GAT		
12–14	3843, 3855, 3875	F:AGT GGG AGT TGT TTG TTA ATT T	59	199
3'CGI shore		R: biotin-AAC CCC ACT CAT AAC TAC AAC ATA		
		S: ATT TTT ATA AGG TTA GTA ATT ATA G		

*Nucleotide number is relative to the ATG start site.

studies varied in design; they used different folate intake doses, time frames and ages of the participants. There are still no studies of gene-specific DNA methylation of genes involved in the transport of folate in the placenta or in leukocytes from subjects with differing levels of Hcy. We hypothesized that aberrant DNA methylation of folate transport genes in the placenta could compromise folate supplies to the embryo, which if occurring at a critical developmental window, could result in an increased risk of NTDs. To test this hypothesis, we developed methods to identify tissue-specific differentially methylated DNA regions (T-DMRs)[16-18] of folate transport genes using pyrosequencing, which is a quantitative and site-specific method. In addition, we explored whether a common polymorphism, *RFC1* 80G > A that abolishes a CpG site in the *RFC1* gene (CpG → CpA), quantitatively affects DNA methylation in its vicinity. We subsequently applied the methods in a clinical study of DNA samples from newborn infants with or without NTDs.

Results

DNA methylation assay development. The folate transport genes *FOLR1*, *PCFT* and *RFC1* have differing CpG site content and distribution. The *FOLR1* gene has the most limited CpG site distribution, while *RFC1* has the broadest. The *PCFT* and *RFC1* genes have more than one CpG island each, and one of them is located at the traditional 5' end of the gene. In contrast, the *FOLR1* gene has one short CpG island located within the coding region of the gene. We designed pyrosequencing methylation assays located in the CpG island and shore regions; the nucleotide positions of analyzed cytosines are defined in **Tables 1, 2 and 3**. A total number of 24 assays covering 121 CpG sites were developed, 5 in the *FOLR1* gene, 8 in the *PCFT* and 11 in the *RFC1* gene. The assay covering CpG sites 50–55 in the *RFC1* gene includes a well-known polymorphism *RFC1* 80G > A (rs 1051266), we therefore also obtained the genotype for this SNP in our DNA samples. The locations of the assays were selected to obtain high quality PCR and sequencing primers. They were tested for potential PCR bias by measuring DNA methylation of standard samples with known percentage methylation and curve analysis of slopes and intercepts. Our assays had curve slope values between 0.93 and 0.98, and intercepts below 12%. Within-assay precision was estimated for CpG sites 3–5 in the *FOLR1* gene, CpG site 45–48 in the *PCFT* gene and 15–17 in the *RFC1* gene. The CV was ≤ 4.4% for all CpG sites analyzed in accordance with a previous study.[19]

Tissue-specific DNA methylation differences and gene expression. The training sets of normal placental tissues and blood leukocytes differed at specific CpG sites, which tended to cluster in different genomic regions. This allowed us to identify T-DMRs, regions with variable and tissue-specific DNA methylation (**Figs. 1–3**). In the *FOLR1* gene, the mean methylated fractions of CpG sites 1–4 and 12–14 flanking the CpG island in the 5' shore and 3' shore regions were statistically significantly ($p < 0.05$) higher in blood leukocytes. In the *PCFT* gene, statistically significantly ($p < 0.05$) higher methylated fractions were found in blood leukocytes in the second CpG island (CGI-2), and in the 3' shore region of the same island, encompassing CpG sites 38–52. In the *RFC1* gene, CpG sites 15–17 in the 5' shore region and sites 18–30 in the CpG island 1 (CGI-1) showed a statistically significant ($p < 0.05$) lower methylated fraction in blood leukocytes. Next, we validated these T-DMRs in the 46 normal placental samples from the test cohort and in 25 leukocyte samples with normal tHcy levels from the training set and obtained results, for the *FOLR1* and *PCFT* genes, that were comparable to those in the training set. In the *RFC1* gene, we obtained 7 additional CpG sites (data not shown).

The mRNA expression of the folate transporter genes *PCFT* and *RFC1* was found to be appreciably lower in the placental

Table 2. PCR primers forward (F), reverse (R) and sequencing primers (S) used for the *PCFT* gene pyrosequencing methylation assays

CpG site no.	Nucleotide no. *	Primer sequence, 5'-3'	T_a (°C)	Size (bp)
1–5	-4604, -4600,-4598	F: GGA AAA GAA AAT TTG TAT TTA GAG TGA GA	57.5	170
5'CGI shore	-4560, -4551	R: biotin-ATC AAA CTA CTA ACC TCA AAT AAT CC		
		S: ATT TGT AAA AAT AAT AAT ATT TGG T		
6–8	-2650, -2616, -2594	F: TTT GGG TTT TGG ATT TTA TAG TGT AG	55	177
5'CGI shore		R: biotin-ACT ACC ATA TCC CCA ACA TCT AAA ATA AT		
		S: TTT TTT TTG AGA TTG AGA GTT		
9–31	-55, -50, -46, -44,	F: GGT GGT TTT AGG TTA TAG G	57.3	366
CGI 1	-42, -37, -34, -30	R: biotin-ATT ACT ACA ACC CCC CCT TTA		
	-23, -14, -11, -9	S1: GTA TAT GGA GGG GAG		
	11, 13, 22, 33, 35	S2: GTT GGT TTT AGG TAG		
	39, 46, 53, 63, 70			
	79			
32–36	276, 287, 295, 304	F: GAG TTT GGT AGG TGG AGG GTT	60	136
CGI 1	318	R: biotin-ATC AAA CCC CTT TAC TCT AAT CCC		
		S: AGG GTT TTG GTT TGG		
38–44	687, 693, 716, 741	F: TTT TTT ATT GGA TTT TTT ATA TGA A	55	147
CGI 2	754, 757, 761, 779	R: biotin-ACA CTA AAA CCT AAA ACA ACA AAC C		
		S1: TTT ATT GGA TTT TTT ATA TG		
		S2: TGT TGG GAG TTT GGA		
45–48	138, 1148, 1153	F: TAT GTA GTT TTT TGT TTT GGT GAG AT	60	177
3'CGI shore	1162	R: biotin-CCC AAA ATA CAC AAT AAT CAC CAC		
		S: GGT GAG ATT TTA AAG GAG TTA		
49–50	2373, 2379	F: GTG TTG GGA TTA TAG GTA TGA GT	60	170
3'CGI shore		R: biotin-AAA ATT CCC TTC TAC TTA ATT ATC AAA C		
		S: GGG ATT ATA GGT ATG AGT TAT		
51–52	3926, 3931	F: AGA TAG AGT AGG GTG AGT GTT AG	59	100
3'CGI shore		R: biotin-ACT ATT CCC CCA ACC ATA AC		
		S: GGT TTT TTA TGT TTA GTG TTG T		

*Nucleotide number is relative to the ATG start site.

tissue than in whole blood leukocytes. In contrast, gene expression of the *FOLR1* gene was much higher in the placental tissue than in leukocytes, see **Table 4**. These expression data are in accordance with annotations in the BioGPS database,[20] see http://biogps.org. Moreover, they suggest an inverse relation between DNA methylation in the T-DMRs of these genes and mRNA levels: The higher folate receptor-α mRNA levels in the placenta mirror inversely the significantly lower DNA methylation in the 5' shore and the 3' shore of the CGI in the *FOLR1* gene (**Fig. 1**), whereas the lower reduced folate carrier-1 mRNA levels in the placenta inversely mirror a significantly higher DNA methylation of the *RFC1* gene in the CGI-1 and its 5' shore (**Fig. 3**). In contrast, the lower proton-coupled folate transporter mRNA levels that were found in placental tissue were not accompanied by any higher DNA methylation of the *PCFT* gene in the 5' region located in the beginning of the CGI-1, which was fully unmethylated in all studied tissues (**Fig. 2**). The statistically significant hypomethylation of the *PCFT* gene that we observed in the placental tissue was located in the CGI-2 and its 3' shore. The functional significance, if any, of this hypomethylation remains unclear.

Methylated fraction in leukocytes from subjects with high or low tHcy and in placental tissue from normal and NTD fetuses. Analysis of methylated fraction of the *RFC1* gene in blood leukocytes revealed site-specific differences ($p < 0.05$) between subjects with low and high tHcy in 17 CpG sites (**Table 5**). In subjects with high tHcy (used as a proxy for poor nutritional status), the methylated fraction was generally lower (14 CpG sites). Most of these sites were found in the 5' shore of the CGI-1, where 7 of the CpG sites differed significantly between the groups ($p < 0.05$). In addition, three CpG sites within the CGI-1 (CpG 18, 21, 25), one CpG site in the 3' shore CGI-1 (CpG 38), and three CpG sites in the CGI-2 (CpG 50, 52 and 55) were significantly lower. Three CpG sites (CpG site 43, 46 and 53) with significantly higher ($p < 0.05$) methylated fraction were also observed, located in the 5' shore and in CGI-2 region, respectively. We did not observe any significant differences between subjects with low or high tHcy in the *FOLR1* or *PCFT* genes. The methylated fraction did

Table 3. PCR primers forward (F), reverse (R) and sequencing primers (S) used for the *RFC1* gene pyrosequencing methylation assays

CpG site No.	Nucleotide No. *	Primer sequence, 5'-3'	T_a (°C)	Size (bp)
1–3	-8067, -8042, -8025	F: GTT AGT GTT GGG AGG TTT GA	59	181
5'CGI shore		R: biotin - TAC AAC TAC CCC TCT CTC CA		
		S: GTT TTT GTG ATG GGT TAT		
4–7	-7784, -7779, -7687, -7773	F: TGG AAA TGT GGG AGG AAA AAT	58	107
5'CGI shore		R: biotin-ACA CCC CAT ATA CAA AAA AAC		
		S: ATT GTA TAT GTT GGG GTA		
8–14	-6224, -6222, -6218	F: TGT GTG GTT GGG GAA TTT T	57	131
5'CGI shore	-6212, -6206, -6202	R: biotin-AAA CCA ATC CCT CAC CTA TCT C		
	-6188	S: AGG GTA GTT TGG GTA GGT TTT T		
15–17	-5456, -6030, -6010	F: GGA AGG GGG TGG GAG TTA T	57	119
5'CGI shore		R: CCA AAA CAA CCT ACT CCC TTT AC		
		S: TTT GTG GGA AGG GGT TTA		
18–23	-5205, -5199, -5193	F: TGG GAG AGT GGT TTA GGT	57	107
CGI 1	-5184, -5182, -5171	R: biotin-AAC CAC CAA TCC CCA TCC		
		S: GTT TTT TTT TTT GAG TGT GAT		
24–30	-3713, -3704, -3693	F: GTG TAA TTT TTT TTT GGA GTA GTT GTG G	57	147
CGI 1	-3688, -3664, -3649	R: biotin-AAC CCT AAA AAA ATA ACT TTC CTA CTA		
	-3629			
		S1: GTG TAA TTT TTT TTT GGA GTA GTT GTG G		
		S2: AGA GAG AGT TTG GAT AG		
31–33	-2989,-2974,-2953	F: TTT GGT TAG TTT TTT AGA GTA GGA GTT G	56	145
3'CGI shore		R: biotin-ACC CCA CTA TCC ACA ATA AC		
		S: GTA GGA GTT GGT TTA AAT		
34–37	-2065, -2079, -2083	F: biotin-ATA GGT TTT GAG GAG GTA TGG	58	148
3'CGI shore	-2092	R: ACA ACC AAA ACC CTA AAA ATT CTC		
		S: AAC CAC TAC CAA ACC		
38–42	-1082, -1067, -1049	F: GTG GTA TTT GGA GAT ATG ATT TTG ATA AGT	57.3	271
5'CGI2 shore	-1037, -1032	R: biotin-ACC CCA AAC CAC AAA ACT TC		
		S: ATT TTG ATA AGT GGA TAG GT		
43–49	-971, -982, -988	F: biotin-TTG GGT AGA ATT AGG ATT GAA AG	57	159
5'CGI2 shore	-950, -939, -930	R: ACC CCA AAC CAC AAA ACT T		
	-918			
		S1: AAT AAA ACA ACA ACA ACA C		
		S2: ACC CAA CCT TAA AAA CC		
50–55	38, 59, 66, 75, 78, 83	F: AGA TTA TTT TTT AAG GTG TTT TGA TTT TAT	57.3	240
CGI 2		R: biotin-AAA ATA ATA AAA CTC TCC CCT AAC C		
		S: GGT GGA GAA GTA GGT G		

*Nucleotide number is relative to the ATG start site.

not differ significantly between placentas from healthy fetuses and from fetuses with NTDs in either of the *FOLR1, PCFT* or *RFC1* genes (**Fig.** 4).

Methylated fraction of CpG sites according to *RFC1* 80G > A genotypes. The genotyping data in subjects with high or low tHcy and placental tissue from normal and NTD subjects are shown in **Table 6**. The *RFC1* polymorphism was in Hardy-Weinberg equilibrium in all subgroups. The genotype distribution did not differ significantly between subjects with low tHcy and high tHcy (χ^2 = 0.199), or between placentas from healthy subjects and those with NTD (χ^2 = 1.77).

The mean methylated fractions of each CpG site in blood leukocytes from subjects with high or low tHcy, grouped according to *RFC1* 80G > A genotype, are shown in **Table 7**. When comparing mean methylated fraction between the genotypes by ANOVA, we did not observe any consistent stepwise gene-dose effect due to the A allele in either high- or low-tHcy subjects (see **Table 7**, p^1 columns). In subjects with low tHcy (used as a proxy

for nutritional sufficiency), only 3 of the 55 CpG sites were significantly differentially methylated (sites 24, 31 and 34, located in the 3' part of the GCI-1). In subjects with high tHcy, the genotype was significantly related to the mean methylated fraction in 4 CpG sites, located at the 5' end of CGI-1 and in the 3' shore of CGI-1 (sites No. 18, 20, 21 and 34); in these subjects, *RFC1* 80AA genotype was associated with a lower methylated fraction compared with the wild-type in 3 of these CpG sites except No. 34 (**Table 7**, right-hand p^1 column).

When the mean methylated fraction in subjects with high or low tHcy was analyzed as dependent variable in a multivariate linear regression model with the group variable (high/low tHcy) and *RFC1* 80G > A genotype as predictors, the group variable was a significant predictor of the mean methylated fraction in a large number of CpG sites (**Table 7**, column p^2), both in the 5' shore (sites No. 3, 6, 8–11, 13 and 15–17), in CGI-1 (sites No. 18–22 and 24–25), the 3' shore (sites No. 31, 34, 38, 43 and 46), and in the 5'-end of CGI-2 (sites No. 50–55). Since we used high tHcy as a proxy for poor nutritional status, this suggests an interaction between nutritional factors and DNA methylation in the *RFC1* gene.

In the NTD placental tissue, we found methylation differences between the *RFC1* 80 G > A genotypes, at CpG sites 8–14, and CpG site 54 (ANOVA, $p < 0.05$, **Fig. 5**). However, there were no statistically significant methylation differences between normal and NTD groups when stratified by genotype (**Fig. 6**).

The *RFC1* 80 G > A genotype status did not affect the methylated fraction of any CpG sites in the *FOLR1* or *PCFT* genes.

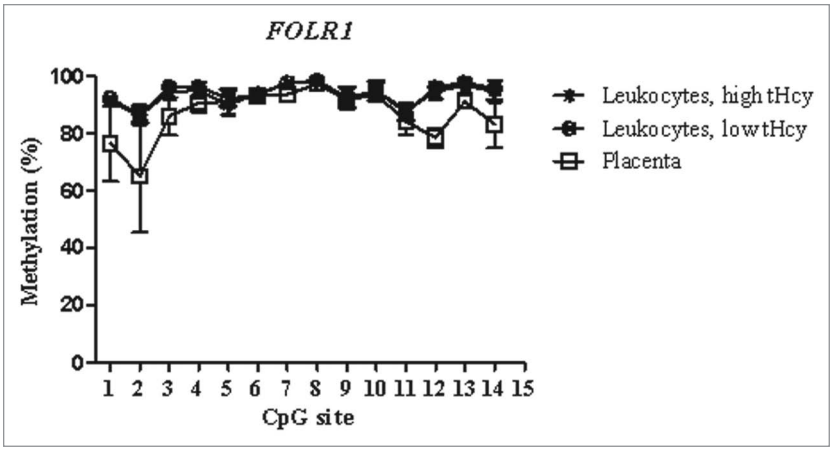

Figure 1. Methylated fraction in the *FOLR1* gene in normal placenta (n = 4), leukocytes from subjects with low tHcy (c = 5–10 μmol/L, n = 24–25), and leukocytes from subjects with high tHcy (c = 20–113 μmol/L, n = 23–25). The error bars show ± 1 SD.

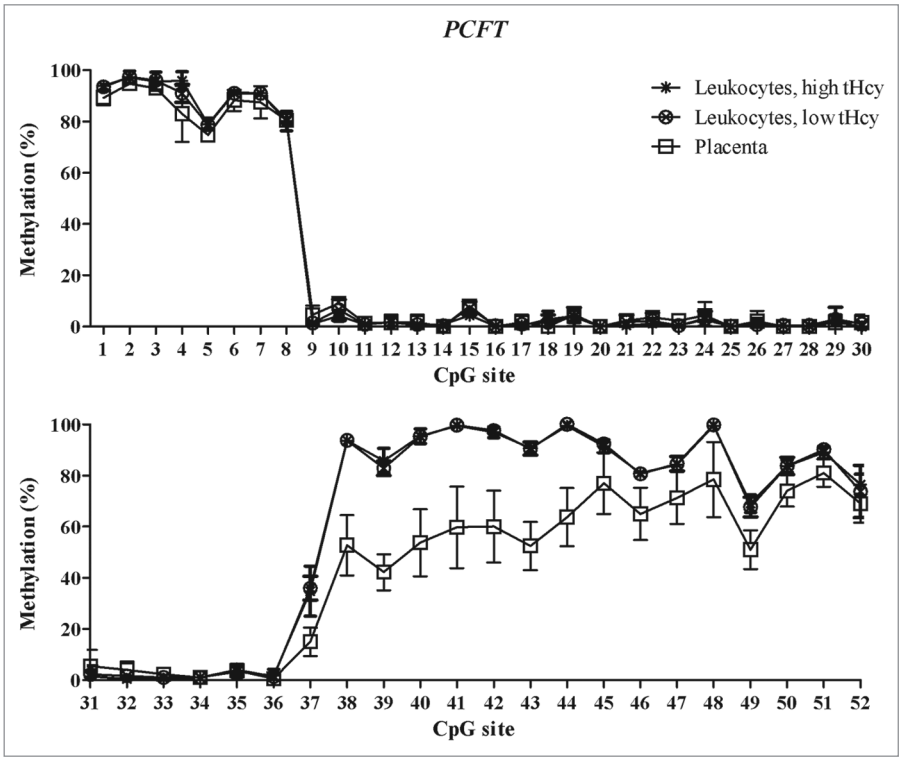

Figure 2. Methylated fraction in the *PCFT* gene in normal placenta (n = 4), leukocytes from subjects with low tHcy (c = 5–10 μmol/L, n = 10–25), and leukocytes from subjects with high tHcy (c = 20–113 μmol/L, n = 11–25). The error bars show ± 1 SD. The upper panel shows CpG sites 1–30 and the lower panel shows CpG sites 31–52.

Discussion

In this study we used a training set of different tissues to locate tissue-specific differentially methylated regions (T-DMRs) in the folate transporter genes *PCFT*, *RFC1* and *FOLR1*. In the clinical study, we found genotype-associated differences in the methylated fraction of the *RFC1* gene in placentas from cases with NTDs, suggestive of a gene-nutrient interaction affecting DNA methylation of this gene in NTD pregnancies, but not in placentas from healthy deliveries.

DNA methylation differences between cancer cells and normal cells have been shown to co-localize with T-DMRs and to occur with higher frequency outside the CpG islands.[17,21,22] We therefore designed our methylation assays to cover both CGIs and CGI shore regions. We found T-DMRs in the CpG island shores of the *FOLR1* gene and in the CGI-2 and 3' shore of the *PCFT* gene (**Figs. 1 and 2**). In the *RFC1* gene, they were located at the 5' shore of CGI-1 and in the CGI-1 (**Fig. 3**). The tissue-specific DNA methylation patterns of these genes indicate that blood leukocytes should not be used routinely as a substitute for other tissues.

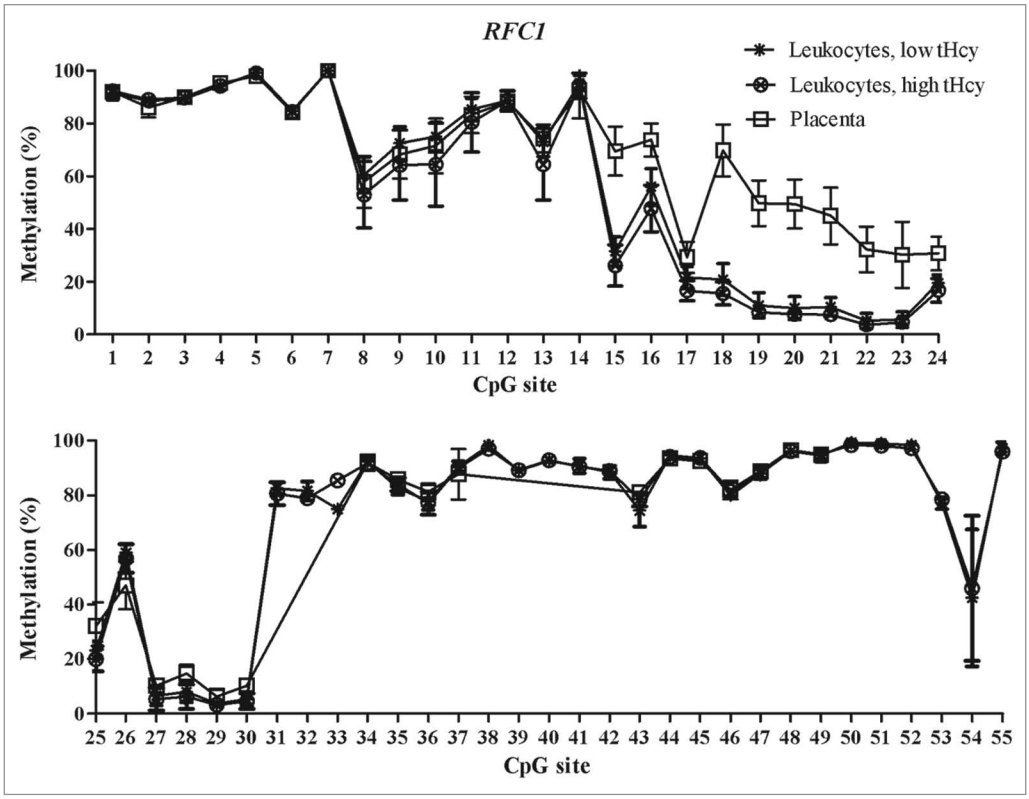

Figure 3. Methylated fraction in the *RFC1* gene in normal placenta (n = 4), leukocytes from subjects with low tHcy (c = 5–10 μmol/L, n = 22–24), and leukocytes from subjects with high tHcy (c = 20–113 μmol/L, n = 21–24). The error bars show ± 1 SD. The upper panel shows CpG sites 1–24 and the lower panel shows CpG sites 25–55.

Table 4. mRNA expression of *FOLR1*, *PCFT* and *RFC1* in full-term placental tissue and whole blood leukocytes

	FOLR1	*PCFT*	*RFC1*
Placental tissue	$1.0 \times 10^{-5} \pm 1.3 \times 10^{-5}$	$1.4 \times 10^{-7} \pm 8.5 \times 10^{-8}$	$5.0 \times 10^{-6} \pm 5.8 \times 10^{-5}$
WBC	$8.4 \times 10^{-8} \pm 1.2 \times 10^{-8}$	$7.4 \times 10^{-6} \pm 1.5 \times 10^{-5}$	$1.3 \times 10^{-4} \pm 2.9 \times 10^{-4}$
Ratio placenta/WBC	119	0.02	0.04

The relative expression was calculated with the ΔCt method ($2^{-\Delta Ct}$), using *18S* as the reference gene.

The relative gene expression of the folate transporter genes showed that *FOLR1* was more abundant in the placental tissue than in leukocytes compared with the *PCFT* and the *RFC1* gene expression, which were less expressed in placenta than in leukocytes. We found an inverse relation between DNA methylation in the T-DMRs of *FOLR1* and *RFC1* and mRNA levels (**Table 4 and Figs. 1–3**). A larger study is warranted to further analyze the correlation between gene expression and DNA methylation of the folate transport genes. Longitudinal studies throughout pregnancy would be highly informative. A study comparing mRNA expression of folate transporter genes between gestational age found lower mRNA expression of the *RFC1* gene in placental tissues from term compared with the 1st trimester, but no DNA methylation data was available.[23]

We detected DNA methylation differences in the *RFC1* gene between subjects with high and low tHcy concentration, but not in the *FOLR1* or *PCFT* genes. This suggests that DNA methylation in the *RFC1* gene may be more sensitive to a deficiency of methyl donors, such as low folate concentrations, than the other genes. In ethanol-induced folate deficient rats, the DNA methylated fraction in CGI of the *RFC1* gene was analyzed, and suggested to be lower compared with the control rats.[24] The mechanism of this ethanol effect is unclear, but it suggests that nutrition may have an impact on the DNA methylation of the *RFC1* gene. Our results showed the greatest difference in methylation in CpG sites in the 5'-shore of the *RFC1* gene: subjects with high tHcy had a lower methylated fraction compared with low tHcy subjects.

The human *RFC1* gene has several promoter regions located ≈4 kB upstream of the transcriptional start site.[25-28] Promoter regions A1/A2, A and B are GC rich, lack TATA boxes, bind Sp transcription factors, and include E-box and Ikaros elements.[25,26] Our assays covering CpG sites 38–42 are located in the promoter region A1/A2, assays including CpG sites 8–14, 18–23 and 24–30 are close to the promoter regions A, B and C. We

Table 5. Mean methylated fraction of CpG sites in the *RFC1* gene in subjects with low or high plasma tHcy concentration

		Low tHcy			High tHcy			
	CpG site*	Mean	SD	N	Mean	SD	N	p
5'shore	8	60.5	6.7	23	53.0	12.5	24	0.037
	9	72.5	6.3	23	64.2	13.2	24	0.022
	10	75.0	5.4	23	64.4	15.7	24	0.009
	13	73.0	5.5	23	64.5	13.6	24	0.017
	15	31.5	5.6	23	26.1	7.8	24	0.030
	16	56.0	7.0	23	47.8	8.9	24	0.002
	17	21.7	4.2	23	16.6	3.9	24	0.000
CGI 1	18	20.9	6.0	24	15.5	4.4	24	0.005
	21	10.5	3.5	24	7.5	1.5	24	0.024
	25	23.3	3.2	24	20.1	4.6	24	0.038
3' shore	38	98.3	1.8	24	97.1	1.7	24	0.029
	43	74.4	5.9	23	78.5	2.6	22	0.010
	46	80.0	1.4	23	81.5	1.8	22	0.032
CGI 2	50	99.3	1.2	22	98.5	1.4	24	0.045
	52	98.5	1.4	22	97.2	1.7	24	0.007
	53	77.1	2.2	22	78.5	1.7	24	0.020
	55	97.3	2.2	22	95.9	1.9	24	0.025

*CpG sites included in the methylation assays, see **Table 3**. Only sites showing statistically significant differences are show in this table. P, post-hoc significance of difference between mean values in leukocytes from subjects with low or high tHcy, respectively.

observed the main difference between subjects with high or low tHcy in the CpG sites 8–17, located upstream of the promoter B region which is also the 5'- shore region related to the CGI-1.

Correlation between DNA methylation in the promoter region of the *RFC1* gene and mRNA expression has been analyzed in various cell lines.[29] In diffuse large B-cell lymphoma cell lines, DNA methylation was suggested to alter mRNA expression, but not in acute lymphoblastic cell lines.[30-32] In contrast to these studies that used qualitative or semi-quantitative assays, we applied quantitative assays to measure DNA methylation in the human folate transport genes.

A crucial question that arises is whether the expression of the three folate transport genes is regulated by methylation in response to folate availability. In order to systematically answer this question, a cohort receiving a controlled folate diet should be analyzed. Regulation of folate transport genes can occur at both the pre- and post-transcriptional levels. Homocysteine itself has been suggested to upregulate the translation of the *FOLR1* receptor.[33] Colon adenoma cancer cells and MCF7 breast cancer cells grown in folate depleted medium showed a reduction of mRNA expression of the *RFC1* gene.[34,35] The authors suggested that it could be a response to prevent efflux of folate through the *RFC1*. Our finding of a higher methylated fraction of the *RFC1* gene in subjects with low tHcy fits with this proposed mechanism of preventing folate-efflux.

The mechanisms by which folate reduces the prevalence of NTDs are still unclear, but it has been confirmed that folic acid consumption by mothers reduces the risk of NTD.[3] Placental tissue express all three folate transport genes, and the suggested metabolic pathway of utilizing Hcy in the placenta is thru the methionine cycle, with folate serving as the methyl donor.[23] We were interested in whether DNA methylation is a potential modulator of folate transport genes in placentas from deliveries of fetuses with NTD. We did not observe any group differences in DNA methylation in *PCFT*, *RFC1* or *FOLR1* genes between placentas from healthy deliveries and those with NTD. If the transport of folate into the cells is defective in NTDs, then the regulation could still be compromised at the mRNA or protein levels, but aberrant DNA methylation of these genes is unlikely to be causative. It would be ideal to explore the effect of DNA methylation in the relevant cell type and at the critical developmental time, in this case neuroepithelial cells and yolk sac cells during the period of neural tube closure, but such collection is ethically and practically undoable and we maintain that the placenta remains a reasonably valid surrogate for the yolk sac in this type of study.

We did observe lower DNA methylated fractions of the *RFC1* gene in placental tissue from infants with NTDs carrying the *RFC1* 80AA genotype when compared with 80GG. Similarly, subjects with high tHcy were found to have lower mean methylated DNA fraction in leukocytes, if they were homozygous for the 80AA allele, than the low tHcy subjects. The importance of the *RFC1* 80G > A polymorphism for plasma tHcy levels has not been clear-cut to date, as some studies showed that AA homozygosity is associated with higher levels of serum folate in women only, while others saw no effect.[36-38] Its association with NTD has also not been consistently reproduced.[39] In a rat model, folate status in females was found to influence the global DNA methylation in placentas by altering the available methyl pool.[40] It is possible that the alteration in methylation status of the *RFC1* gene epigenetically impacts

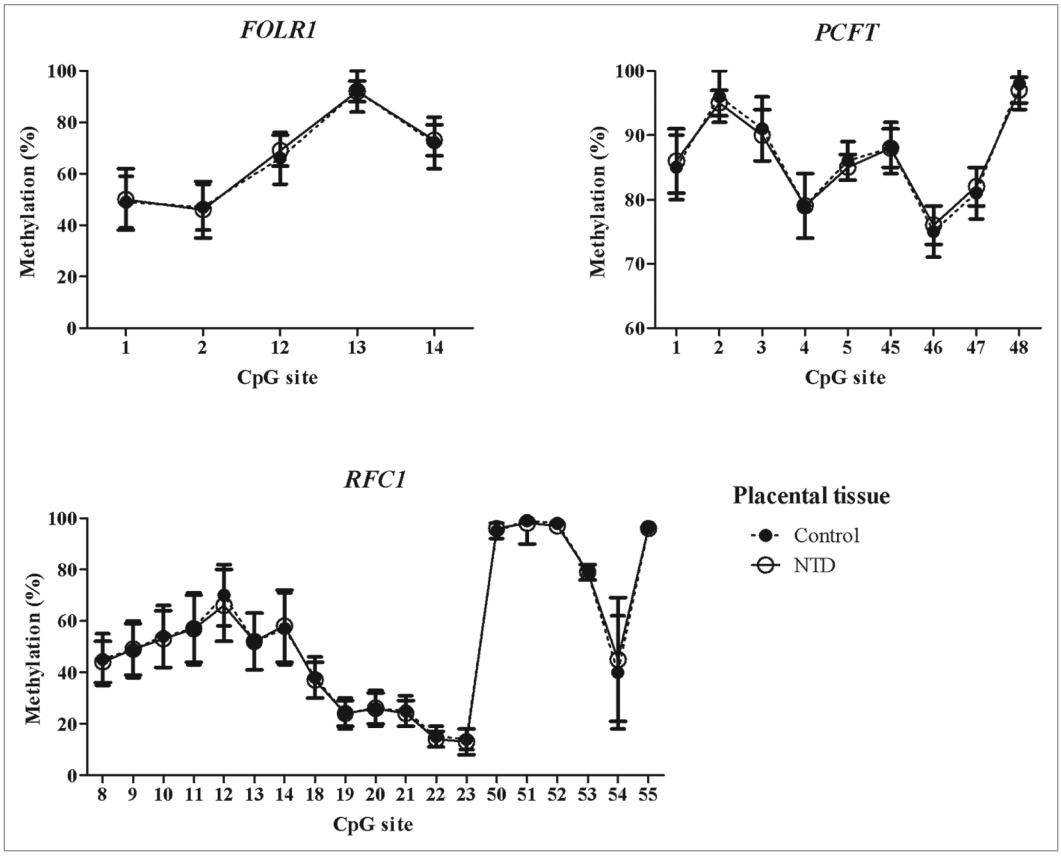

Figure 4. Methylated fraction in the *FOLR1*, *PCFT* and *RFC1* gene in placental tissue from healthy (n = 39–48) and NTD (n = 66–75) subjects. The error bars show ± 1 SD.

Table 6. *RFC1* 80G > A genotype prevalence and allele frequencies in subjects with low and high tHcy and normal and NTD subjects

	Leucocytes				Placenta			
	Low tHcy		High tHcy		Normal		NTD	
***RFC1* 80G > A**	n	%	n	%	n	%	n	%
GG	6	(27)	8	(33)	8	(21)	22	(32)
GA	12	(54)	12	(50)	23	(61)	33	(49)
AA	4	(18)	4	(17)	7	(18)	13	(19)
Total	22		24		38		68	
	$\chi^2 = 0.22$		$\chi^2 = 0.02$		$\chi^2 = 1.7$		$\chi^2 = 0.01$	
p(G)	0.583		0.545		0.513		0.566	
q(A)	0.417		0.454		0.487		0.434	

its pattern of expression in such a way as to impair normal neural tube closure. If the folate transport genes simply moved molecules of one carbon donors into and out of cells, that would be one way in which to envision a mechanism underlying NTD formation. However, there is every likelihood that these transport proteins have a cell signaling function which is every bit as important in regulating critical signal transduction events during neurulation. Altering the expression of *RFC1* is perhaps only an initiating step in impacting a network of genes involved in cell morphogenetic movements that are essential to completing neural tube closure. We do not rule out that DNA methylation changes in other one-carbon metabolism genes or planar cell polarity genes may be contributing, perhaps in interaction with DNA methylation changes in folate transport genes, to an increased NTD risk, but we are filling a significant data gap on T-DMRs in folate transport genes.

In conclusion, we have identified tissue-specific differentially methylated DNA regions (T-DMRs) in three folate transport genes, and shown an inverse relation between methylation and mRNA abundance for the *FOLR1* and *RFC1* genes. *RFC1* mean methylated fraction was found to depend on the *RFC1* 80G > A genotype in subjects with high tHcy, used as a proxy for poor nutritional status, and in placentas from NTD subjects. We therefore postulate a gene-nutrition interaction between folate intake, *RFC1* genotype, *RFC1* DNA methylation, and *RFC1* mRNA transcription, which could account for part of the spectrum of NTD births. Recognition of this interaction in future research may lead to a fuller appreciation of the role of the folate receptors in the etiology of NTDs.

Material and Methods

Study population. A training set consisting of 56 discarded blood samples and four placental tissues collected from our

Table 7. Methylated fraction of CpG sites in the *RFC1* gene in blood leukocytes form subjects with low and high tHcy according to genotype

		Low tHcy				High tHcy				
CpG site	**Genotype**	**Mean**	**SD**	**N**	**p[1]**	**Mean**	**SD**	**N**	**p[1]**	**p[2]**
CpG 3	GG	89.3	0.5	6		89.9	0.6	8		
	GA	89.3	0.7	12		89.8	0.8	12		
	AA	89.0	0.8	4	0.656	90.0	0.8	4	0.823	0.006
CpG 6	GG	85.3	0.8	6		83.7	1.0	7		
	GA	84.7	1.3	12		85.0	1.1	12		
	AA	85.3	0.5	4	0.415	84.3	1.5	4	0.079	0.046
CpG 8	GG	56.8	8.6	6		50.3	11.4	8		
	GA	61.0	6.2	12		56.3	8.5	12		
	AA	61.0	1.0	3	0.448	48.5	23.2	4	0.434	0.029
CpG 9	GG	68.0	7.6	6		60.4	11.2	8		
	GA	73.2	5.2	12		68.1	8.8	12		
	AA	73.3	0.6	3	0.195	60.3	25.3	4	0.372	0.020
CpG 10	GG	72.2	7.6	6		58.8	16.1	8		
	GA	75.6	4.5	12		69.5	9.4	12		
	AA	76.0	3.6	3	0.432	60.5	27.4	4	0.291	0.007
CpG 11	GG	83.5	4.9	6		80.3	10.5	8		
	GA	85.5	4.5	12		82.6	6.8	12		
	AA	86.3	1.5	3	0.578	74.3	21.5	4	0.454	0.049
CpG 13	GG	69.5	6.4	6		59.5	14.5	8		
	GA	73.5	5.3	12		68.8	7.9	12		
	AA	74.0	0.0	3	0.307	61.3	23.1	4	0.293	0.014
CpG 15	GG	26.6	2.1	5		26.1	7.1	8		
	GA	33.2	6.3	12		27.8	7.5	12		
	AA	32.5	5.4	4	0.099	21.3	10.2	4	0.370	0.016
CpG 16	GG	52.2	4.4	5		46.9	7.8	8		
	GA	56.3	7.6	12		50.4	7.0	12		
	AA	59.5	8.7	4	0.332	41.8	14.4	4	0.233	0.001
CpG 17	GG	19.2	1.6	5		16.1	2.9	8		
	GA	22.3	4.9	12		18.1	3.7	12		
	AA	22.3	4.4	4	0.407	13.3	4.3	4	0.080	0.000
CpG 18	GG	16.2	2.6	6		15.1	4.1	8		
	GA	22.3	6.4	12		17.4	2.8	12		
	AA	23.5	7.2	4	0.089	10.8	5.7	4	0.021	0.000
CpG 19	GG	8.8	1.6	6		8.5	2.2	8		
	GA	11.3	5.9	12		9.2	1.7	12		
	AA	13.5	4.8	4	0.350	6.3	2.8	4	0.070	0.011
CpG 20	GG	8.0	1.4	6		7.6	2.0	8		
	GA	10.1	5.5	12		8.5	1.9	12		
	AA	12.3	4.4	4	0.370	5.3	2.8	4	0.042	0.012
CpG 21	GG	8.2	1.2	6		7.4	1.2	8		
	GA	11.2	4.1	12		8.3	1.1	12		

p[1] difference between mean methylated fraction in subjects with different RFC1 80G > A genotypes. p[2] difference between mean methylated fraction in subjects with high or low tHcy concentration, adjusted for RFC1 80G > A genotype. Please refer to the Statistics section for details of the multivariate model used.

Table 7. Methylated fraction of CpG sites in the *RFC1* gene in blood leukocytes form subjects with low and high tHcy according to genotype (continued)

CpG site	Genotype	Mean	SD	N	p[1]	Mean	SD	N	p[1]	p[2]
			Low tHcy				High tHcy			
	AA	11.8	3.8	4	0.190	5.8	1.9	4	0.008	0.000
CpG 22	GG	3.3	0.5	6		3.3	1.6	8		
	GA	5.6	3.1	12		4.3	0.9	12		
	AA	6.5	2.4	4	0.132	2.8	1.3	4	0.052	0.012
CpG 24	GG	17.2	3.0	6		14.8	3.5	8		
	GA	21.2	2.8	12		18.8	4.8	12		
	AA	19.3	2.1	4	0.028	14.5	3.3	4	0.081	0.009
CpG 25	GG	21.3	2.9	6		18.1	4.8	8		
	GA	24.3	3.4	12		21.6	4.1	12		
	AA	22.8	1.7	4	0.186	19.8	5.1	4	0.265	0.026
CpG 31	GG	80.5	3.3	6		78.9	4.6	8		
	GA	83.0	1.1	12		81.8	3.7	12		
	AA	84.3	2.1	4	0.025	80.5	4.5	4	0.313	0.051
CpG 34	GG	91.0	1.2	4		90.0	1.3	6		
	GA	92.8	0.9	10		92.2	1.4	11		
	AA	93.3	1.0	4	0.010	93.3	1.9	4	0.006	0.232
CpG 38	GG	98.7	1.2	6		96.6	2.0	8		
	GA	98.2	1.7	12		97.4	1.7	12		
	AA	98.5	2.4	4	0.833	97.0	1.6	4	0.627	0.017
CpG 43	GG	73.4	8.3	5		77.8	2.9	6		
	GA	76.7	4.0	12		78.6	2.7	12		
	AA	71.3	6.4	4	0.228	79.3	1.7	4	0.703	0.003
CpG 46	GG	80.4	1.8	5		81.0	0.6	6		
	GA	79.8	1.4	12		81.1	1.4	12		
	AA	80.5	1.3	4	0.583	83.3	3.3	4	0.093	0.007
CpG 50	GG	99.7	0.8	6		98.4	1.4	8		
	GA	99.2	1.3	12		98.7	1.6	12		
	AA	99.0	1.4	4	0.646	98.0	1.4	4	0.730	0.044
CpG 51	GG	99.5	0.5	6		98.0	1.3	8		
	GA	98.6	1.4	12		98.2	1.6	12		
	AA	99.5	1.0	4	0.230	98.8	1.5	4	0.710	0.052
CpG 52	GG	98.0	1.7	6		97.0	1.5	8		
	GA	98.4	1.4	12		97.4	1.8	12		
	AA	99.3	1.0	4	0.402	96.8	1.7	4	0.756	0.006
CpG 53	GG	76.8	2.9	6		78.1	1.5	8		
	GA	77.3	2.1	12		78.6	1.8	12		
	AA	77.0	1.6	4	0.902	79.0	1.4	4	0.675	0.024
CpG 54	GG	76.2	2.6	6		77.9	1.1	8		
	GA	38.8	1.9	12		39.2	1.6	12		
	AA	3.3	1.0	4	0.000	2.5	0.6	4	0.000	0.417
CpG 55	GG	98.2	1.9	6		96.3	2.4	8		
	GA	97.0	2.5	12		96.0	1.7	12		
	AA	97.0	1.6	4	0.568	95.0	1.4	4	0.565	0.021

p[1] difference between mean methylated fraction in subjects with different RFC1 80G > A genotypes. p[2] difference between mean methylated fraction in subjects with high or low tHcy concentration, adjusted for RFC1 80G > A genotype. Please refer to the Statistics section for details of the multivariate model used.

routine clinical activities (Dept. of Laboratory Medicine, Örebro University Hospital) was used for method development purposes and to identify regions of differential DNA methylation. We selected and de-identified 25 blood samples with tHcy in the range of 5–10 μmol/L (serving as a proxy to define presumably well-nourished subjects), 25 blood samples in the range of 20–113 μmol/L (serving as a proxy to define presumably poorly nourished subjects), in the following designated "low tHcy" and "high tHcy" respectively, and finally, four de-identified placental tissues collected immediately after uncomplicated vaginal delivery. The testing cohort consisted of placental tissues from deliveries of healthy fetuses (n = 48) or fetuses with neural tube defects (n = 75), collected with appropriate informed consent in Shanxi Province, China. All clinical samples were obtained with appropriate IRB approval. The Regional Ethics Review Board, Uppsala, approved the Swedish part of the project.

DNA extraction, bisulphite treatment. Genomic DNA was extracted from 200 μL whole EDTA blood using QIAamp EZ1 DNA blood 200 μl Kit according to the manufacturer's instruction (Qiagen Inc.) utilizing a BioRobot EZ1 (Qiagen Inc.). Genomic DNA from placental tissue was manually extracted with Gentra PureGene or QIAmp DNA mini kit (Qiagen Inc.). Approximately 1,000 ng extracted DNA was used for the bisulphite treatment performed with EZ DNA Methylation Gold kit according to the instructions by the manufacturer and eluted in 25 μL elution buffer (Zymo Research, Orion Diagnostica).

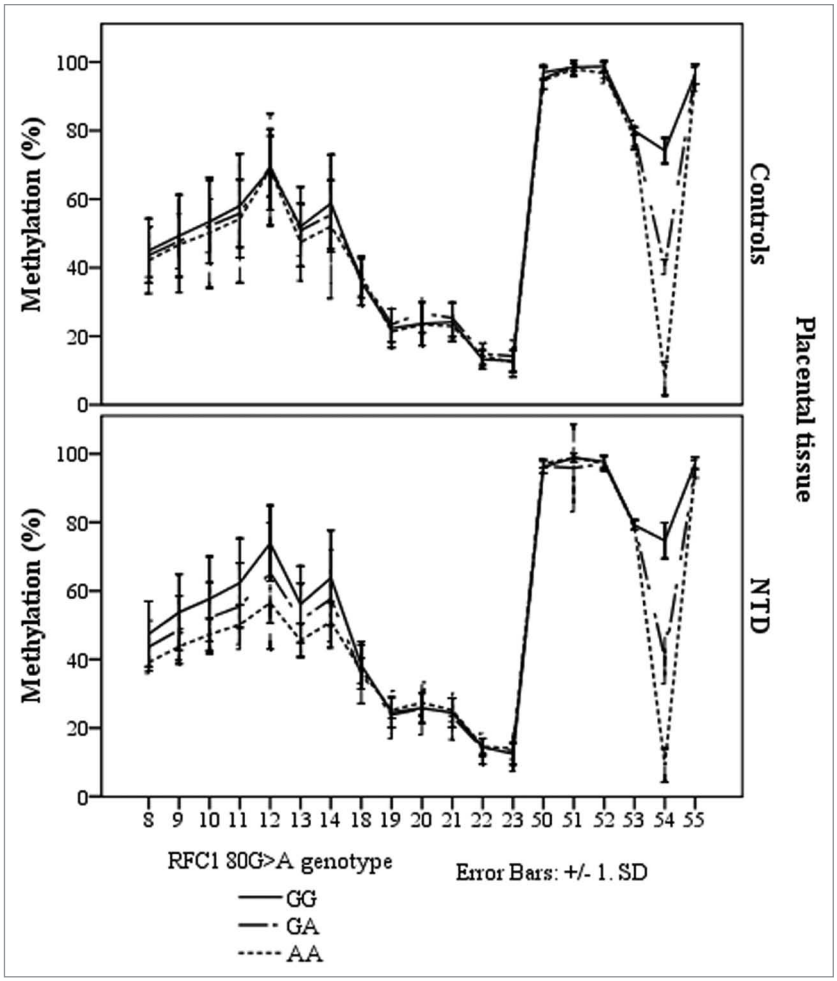

Figure 5. Methylated fraction in the *RFC1* gene according to *RFC1* 80G > A genotype in placentas, stratified by groups of healthy controls (n = 38) and NTD (n = 68). The error bars show ± 1 SD.

mRNA extraction and quantitative real-time PCR (qPCR). Expression analysis of the folate transporters was performed from the training set tissues of four placental tissues and six healthy normal blood donors. RNA was extracted from 4 placental tissues with a standard TRIzol RNA extraction protocol (TRIzol® Reagent). Extractions from whole blood samples were made with the QIAmp RNA Blood Mini Kit (QIAGEN Inc.).

qPCR was performed with an ABI 7500 Fast Real-Time PCR system (Applied Biosystems) according to the manufacturer's instructions. All samples and negative controls were run as triplicates and the qPCR protocol was as follows. The baseline was set between 3–15 cycles and the threshold to 0.2, a total of 50 cycles was run.

Gene expression assays for the folate receptor α (*FOLR1,* hs01124177_m1) and 18S (Hs99999901_s1) were purchased from Applied Biosystems. Assays for: *SLC46A1*, proton coupled folate transporter (*PCFT*), and *SLC19A1*, reduced folate carrier (*RFC1*) were designed in-house, with the Primer Express 3.0 software (Applied Biosystems) see **Table 8** for details. All in-house assays are labeled with Fam-Tamra dyes and were purchased from www.biomers.net (Ulm/Donau). Normalization was performed with *18S* using the ΔCt-method.[41]

Methylation assay development and PCR amplification. Prior to primer design, we used the online web tool CpG island searcher (http://cpgislands.usc.edu/) to locate the CpG sites and putative CpG islands (CGI). We used the nucleotide sequence GenBank U20391.1 for the *FOLR1* gene and Ensemble sequence ENSG00000076351 for the *PCFT* gene, including an additional 5,000 bp upstream of the 5' end of the gene. The *RFC1* genomic sequence and 3861 bp up-stream of the 5' end was obtained from Ensemble (ENSG00000173638), and was used for the development of the methylation assays. Regions of interest were located and primers were designed using Pyromark assay design software 2.0 (Qiagen). Touch-down PCR has been recommended for amplifying bisulphite treated DNA and was used here.[42] The PCR program was as follows: initial denaturation step of 5 min at 95°C, followed by 12 cycles of 30 sec denaturation at 94°C, 45 sec of varying annealing temperature (T_a + 10°C, decreasing 1°C each cycle) and extension of 45 sec at 72°C. Further 40 cycles were as follows: denaturation of 30 sec at 94°C, specific

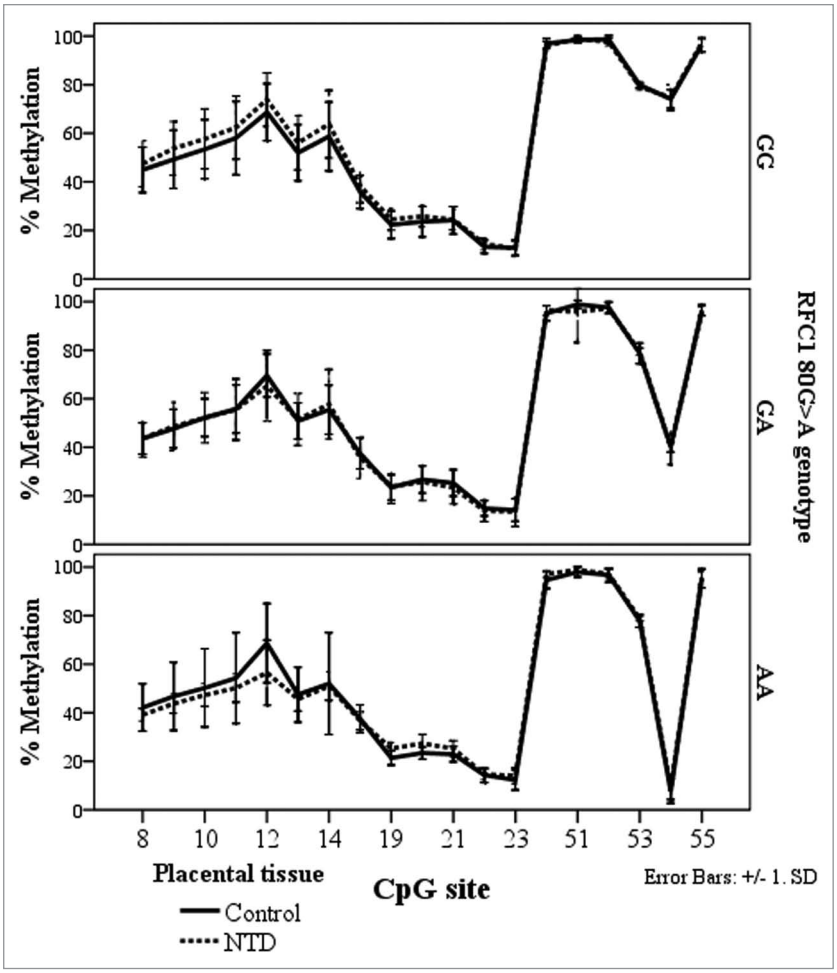

Figure 6. Methylated fraction in the *RFC1* gene in placentas of normal control births (n = 38) and NTD births (n = 68) stratified by *RFC1* 80G > A genotype.

Table 8. In-house design of mRNA expression assays for the *PCFT* and *RFC1* genes

Gene		Sequence 5'–3'	Size (bp)
RFC1	Fw	CGT CAA GAC CAT CAT CAC TTT CA	100
	Rev	CAG GAT CAG GAA GTA CAC GGA GTA	
	Pr	CCG GTC CGC AAG CAG TTC CAG TT	
PCFT	Fw	TTC ACA GGA TAT GGG TTG CTT TT	120
	Rev	CAC ACA GGC CAC AGC AGA AA	
	Pr	CTG TCA TCC GGG CTA AAC TCT CCA AGC T	

Fw, forward primer; Rw, reverse primer; Pr, probe.

annealing T_a for 45 sec and extension for 45 sec at 72°C and one cycle for 7 min at 72°C. 40 μL PCR reaction was performed with the HotStarTaq DNA Polymerase Kit (QIAGEN Inc.), containing 0.15 μmol/L of each primer, 1.25 unit of Taq polymerase, 1.5–3.0 mM $MgCl_2$, and 0.1 mM each of dGTP, dATP, dTTP, dCTP and 30 ng of bisulphite treated DNA was added as template. The PCR primers, annealing temperatures, and amplicon sizes are shown in **Tables 1–3**. All primers were purchased from www.biomers.net (Ulm/Donau).

To detect biased amplification of the un-methylated allele, we performed a titration assay on samples with known methylation levels of 0%, 10%, 25%, 50%, 85% and 100% methylation.[43] Synthetically methylated and non-methylated DNA standards were purchased from Zymo Research (Orion Diagnostica) and Qiagen. The standards were mixed to obtain the percentages of methylation for titration and used in subsequent bisulfite- PCR- and pyrosequencing reactions.

Pyrosequencing. To obtain a quantitative measure of site-specific methylation, the CpG sites were analyzed using Pyrosequencing® technology. Following PCR (see above, and **Tables 1–3**), the samples were prepared using the Vacuum Prep Workstation (Qiagen): 25–30 μL of the amplicon, 3 μL Streptavidin Sepharose HP Beads (Amersham Biosciences), 37 μL binding buffer (10 mmol/L TRIS-HCl, 2 mol/L NaCl, 1 mmol/L EDTA, 0.1% Tween 20, Milli-Q (18.2 MΩ × cm) water, pH 7.6) and 10–15 μL Milli-Q water were mixed and used in the Vacuum Prep workstation. The biotinylated amplicons were immobilized onto the Streptavidin sepharose beads and then passed through one denaturation and two washing steps using the Vacuum Prep Workstation according to a standard protocol. The amplicons were subsequently transferred to a plate containing sequencing primer (0.4 μmol/L) in 40 μL annealing buffer (20 mmol/L Tris-Acetate, 2 mmol/L Magnesium acetate, pH 7.6). Sequencing was performed using a Pyromark Gold Q96 Reagent Kit and a PSQ 96ID system (Qiagen). The nucleotide addition order was optimized by the Pyro Q-CpG software version 1.0.9 (Qiagen). Results were automatically analyzed using the same software.

Assay precision. To determine the precision of the method we studied CpG sites 3–5 in the *FOLR1* gene, CpG sites 45–48 in the *PCFT* gene and sites 15–17 in the *RFC1* gene. One leukocyte DNA sample was bisulphite treated 8 times. Each aliquot was then PCR amplified three times and analyzed by pyrosequencing. The CV of the assays was calculated as the standard deviation divided by the mean value for each separate CpG site.

Statistical analysis. Means were compared using ANOVA. The Hardy-Weinberg equilibrium of genotypes was tested with χ^2 test and performed for subjects within a specific group. The statistical significance of 80G > A genotype and of study group (subjects with high or low tHcy, respectively) as determinants of the mean methylated fraction of CpG sites was tested in a general linear model, with *RFC1* genotype and study group as fixed factors and methylated fraction as dependent variable. All calculations were performed by the SPSS software version 15.0 (SPSS Inc.).

Disclosure of Potential Conflicts of Interest

No potential conflicts of interest were disclosed.

Acknowledgments

Financial support by Lions cancerfond, Nyckelfonden, and Örebro läns landsting is gratefully acknowledged. RHF was supported in part by NIH grants HD067244 and ES021390. AR was supported in part by a grant from the State Key Development Program for Basic Research (2007CB5119001), People's Republic of China.

Financial Disclosures

S.A.F., A.K.B., H.S.I. and T.K.N. were supported by Lions cancerfond, Nyckelfonden and Örebro läns landsting. RHF was supported in part by NIH grants HD067244 and ES021390. A.R. was supported in part by a grant from the State Key Development Program for Basic Research (2007CB5119001), People's Republic of China.

References

1. Blom HJ, Smulders Y. Overview of homocysteine and folate metabolism. With special references to cardiovascular disease and neural tube defects. J Inherit Metab Dis 2011; 34:75-81; PMID:20814827; http://dx.doi.org/10.1007/s10545-010-9177-4.
2. Tibbetts AS, Appling DR. Compartmentalization of Mammalian folate-mediated one-carbon metabolism. Annu Rev Nutr 2010; 30:57-81; PMID:20645850; http://dx.doi.org/10.1146/annurev.nutr.012809.104810.
3. Blom HJ. Folic acid, methylation and neural tube closure in humans. Birth Defects Res A Clin Mol Teratol 2009; 85:295-302; PMID:19301298; http://dx.doi.org/10.1002/bdra.20581.
4. Jacob RA, Wu MM, Henning SM, Swendseid ME. Homocysteine increases as folate decreases in plasma of healthy men during short-term dietary folate and methyl group restriction. J Nutr 1994; 124:1072-80; PMID:8027858.
5. Zhao R, Diop-Bove N, Visentin M, Goldman ID. Mechanisms of Membrane Transport of Folates into Cells and Across Epithelia. Annual Review of Nutrition, Vol 31 2011; 31:177-201.
6. Saitsu H, Ishibashi M, Nakano H, Shiota K. Spatial and temporal expression of folate-binding protein 1 (Fbp1) is closely associated with anterior neural tube closure in mice. Dev Dyn 2003; 226:112-7; PMID:12508232; http://dx.doi.org/10.1002/dvdy.10203.
7. Yasuda S, Hasui S, Yamamoto C, Yoshioka C, Kobayashi M, Itagaki S, et al. Placental folate transport during pregnancy. Biosci Biotechnol Biochem 2008; 72:2277-84; PMID:18776693; http://dx.doi.org/10.1271/bbb.80112.
8. Spiegelstein O, Mitchell LE, Merriweather MY, Wicker NJ, Zhang Q, Lammer EJ, et al. Embryonic development of folate binding protein-1 (Folbp1) knockout mice: Effects of the chemical form, dose, and timing of maternal folate supplementation. Dev Dyn 2004; 231:221-31; PMID:15305303; http://dx.doi.org/10.1002/dvdy.20107.
9. Piedrahita JA, Oetama B, Bennett GD, van Waes J, Kamen BA, Richardson J, et al. Mice lacking the folic acid-binding protein Folbp1 are defective in early embryonic development. Nat Genet 1999; 23:228-32; PMID:10508523; http://dx.doi.org/10.1038/13861.
10. Tang LS, Finnell RH. Neural and orofacial defects in Folbp1 knockout mice. Birth Defects Research Part a-Clinical and Molecular Teratology 2003; 67.
11. Tang LS, Wlodarczyk BJ, Santillano DR, Miranda RC, Finnell RH. Developmental consequences of abnormal folate transport during murine heart morphogenesis. Birth Defects Research Part a-Clinical and Molecular Teratology 2004; 70.
12. Zhu H, Wlodarczyk BJ, Scott M, Yu W, Merriweather M, Gelineau-van Waes J, et al. Cardiovascular abnormalities in Folr1 knockout mice and folate rescue. Birth Defects Research Part a-Clinical and Molecular Teratology 2007; 79.
13. Boyles AL, Ballard JL, Gorman EB, McConnaughey DR, Cabrera RM, Wilcox AJ, et al. Association between inhibited binding of folic acid to folate receptor alpha in maternal serum and folate-related birth defects in Norway. Hum Reprod 2011; 26:2232-8; PMID:21576080; http://dx.doi.org/10.1093/humrep/der144.
14. Esteller M. Human Cancer Epigenetics. European Journal of Cancer 2011; 47:S25-S; http://dx.doi.org/10.1016/S0959-8049(11)70311-2.
15. Terry MB, Delgado-Cruzata L, Vin-Raviv N, Wu HC, Santella RM. DNA methylation in white blood cells: association with risk factors in epidemiologic studies. Epigenetics 2011; 6:828-37; PMID:21636973; http://dx.doi.org/10.4161/epi.6.7.16500.
16. Saied MH, Marzec J, Khalid S, Smith P, Down TA, Rakyan VK, et al. Genome wide analysis of acute myeloid leukemia reveal leukemia specific methylome and subtype specific hypomethylation of repeats. PLoS One 2012; 7:e33213; PMID:22479372; http://dx.doi.org/10.1371/journal.pone.0033213.
17. Irizarry RA, Ladd-Acosta C, Wen B, Wu Z, Montano C, Onyango P, et al. The human colon cancer methylome shows similar hypo- and hypermethylation at conserved tissue-specific CpG island shores. Nat Genet 2009; 41:178-86; PMID:19151715; http://dx.doi.org/10.1038/ng.298.
18. Doi A, Park IH, Wen B, Murakami P, Aryee MJ, Irizarry R, et al. Differential methylation of tissue- and cancer-specific CpG island shores distinguishes human induced pluripotent stem cells, embryonic stem cells and fibroblasts. Nat Genet 2009; 41:1350-3; PMID:19881528; http://dx.doi.org/10.1038/ng.471.
19. Löf-Ohlin ZM, Nilsson TK. Pyrosequencing assays to study promoter CpG site methylation of the O6-MGMT, hMLH1, p14ARF, p16INK4a, RASSF1A, and APC1A genes. Oncol Rep 2009; 21:721-9; PMID:19212632.
20. Wu C, Orozco C, Boyer J, Leglise M, Goodale J, Batalov S, et al. BioGPS: an extensible and customizable portal for querying and organizing gene annotation resources. Genome Biol 2009; 10:R130; PMID:19919682; http://dx.doi.org/10.1186/gb-2009-10-11-r130.
21. Eckhardt F, Lewin J, Cortese R, Rakyan VK, Attwood J, Burger M, et al. DNA methylation profiling of human chromosomes 6, 20 and 22. Nat Genet 2006; 38:1378-85; PMID:17072317; http://dx.doi.org/10.1038/ng1909.
22. Shiota K, Kogo Y, Ohgane J, Imamura T, Urano A, Nishino K, et al. Epigenetic marks by DNA methylation specific to stem, germ and somatic cells in mice. Genes Cells 2002; 7:961-9; PMID:12296826; http://dx.doi.org/10.1046/j.1365-2443.2002.00574.x.
23. Solanky N, Requena Jimenez A, D'Souza SW, Sibley CP, Glazier JD. Expression of folate transporters in human placenta and implications for homocysteine metabolism. Placenta 2010; 31:134-43; PMID:20036773; http://dx.doi.org/10.1016/j.placenta.2009.11.017.
24. Wani NA, Nada R, Kaur J. Biochemical and molecular mechanisms of folate transport in rat pancreas; interference with ethanol ingestion. PLoS One 2011; 6:e28599; PMID:22163044; http://dx.doi.org/10.1371/journal.pone.0028599.
25. Whetstine JR, Matherly LH. The basal promoters for the human reduced folate carrier gene are regulated by a GC-box and a cAMP-response element/AP-1-like element. Basis for tissue-specific gene expression. J Biol Chem 2001; 276:6350-8; PMID:11078737; http://dx.doi.org/10.1074/jbc.M008074200.
26. Liu MJ, Whetstine JR, Payton SG, Ge Y, Flatley RM, Matherly LH. Roles of USF, Ikaros and Sp proteins in the transcriptional regulation of the human reduced folate carrier B promoter. Biochem J 2004; 383:249-57; PMID:15214842; http://dx.doi.org/10.1042/BJ20040414.
27. Whetstine JR, Flatley RM, Matherly LH. The human reduced folate carrier gene is ubiquitously and differentially expressed in normal human tissues: identification of seven non-coding exons and characterization of a novel promoter. Biochem J 2002; 367:629-40; PMID:12144527; http://dx.doi.org/10.1042/BJ20020512.
28. Payton SG, Liu MJ, Ge YB, Matherly LH. Transcriptional regulation of the human reduced folate carrier A1/A2 promoter: Identification of critical roles for the USF and GATA families of transcription factors. Biochim Biophys Acta 2005; 1731:115-24; PMID:16225938; http://dx.doi.org/10.1016/j.bbaexp.2005.08.010.
29. Yang R, Li WW, Hoang BH, Kim H, Banerjee D, Kheradpour A, et al. Quantitative correlation between promoter methylation and messenger RNA levels of the reduced folate carrier. BMC Cancer 2008; 8:8; PMID:18194582.
30. Kastrup IB, Worm J, Ralfkiaer E, Hokland P, Guldberg P, Grønbaek K. Genetic and epigenetic alterations of the reduced folate carrier in untreated diffuse large B-cell lymphoma. Eur J Haematol 2008; 80:61-6; PMID:18028428.
31. Liu MJ, Ge YB, Payton SG, Aboukameel A, Buck S, Flatley RM, et al. Transcriptional regulation of the human reduced folate carrier in childhood acute lymphoblastic leukemia cells. Clin Cancer Res 2006; 12:608-16; PMID:16428507; http://dx.doi.org/10.1158/1078-0432.CCR-05-1954.
32. Rothem L, Stark M, Kaufman Y, Mayo L, Assaraf YG. Reduced folate carrier gene silencing in multiple antifolate-resistant tumor cell lines is due to a simultaneous loss of function of multiple transcription factors but not promoter methylation. J Biol Chem 2004; 279:374-84; PMID:14551190; http://dx.doi.org/10.1074/jbc.M309092200.
33. Antony AC, Tang YS, Khan RA, Biju MP, Xiao XL, Li QJ, et al. Translational upregulation of folate receptors is mediated by homocysteine via RNA-heterogeneous nuclear ribonucleoprotein E1 interactions. J Clin Invest 2004; 113:285-301; PMID:14722620.

34. Hayashi I, Sohn KJ, Stempak JM, Croxford R, Kim YI. Folate deficiency induces cell-specific changes in the steady-state transcript levels of genes involved in folate metabolism and 1-carbon transfer reactions in human colonic epithelial cells. J Nutr 2007; 137:607-13; PMID:17311948.
35. Ifergan I, Jansen G, Assaraf YG. The reduced folate carrier (RFC) is cytotoxic to cells under conditions of severe folate deprivation. RFC as a double edged sword in folate homeostasis. J Biol Chem 2008; 283:20687-95; PMID:18499665; http://dx.doi.org/10.1074/jbc.M802812200.
36. Devlin AM, Clarke R, Birks J, Evans JG, Halsted CH. Interactions among polymorphisms in folate-metabolizing genes and serum total homocysteine concentrations in a healthy elderly population. Am J Clin Nutr 2006; 83:708-13; PMID:16522921.
37. Stanisławska-Sachadyn A, Mitchell LE, Woodside JV, Buckley PT, Kealey C, Young IS, et al. The reduced folate carrier (SLC19A1) c.80G>A polymorphism is associated with red cell folate concentrations among women. Ann Hum Genet 2009; 73:484-91; PMID:19650776; http://dx.doi.org/10.1111/j.1469-1809.2009.00529.x.
38. Chango A, Emery-Fillon N, de Courcy GP, Lambert D, Pfister M, Rosenblatt DS, et al. A polymorphism (80G->A) in the reduced folate carrier gene and its associations with folate status and homocysteinemia. Mol Genet Metab 2000; 70:310-5; PMID:10993718; http://dx.doi.org/10.1006/mgme.2000.3034.
39. Greene NDE, Stanier P, Copp AJ. Genetics of human neural tube defects. Hum Mol Genet 2009; 18(R2):R113-29; PMID:19808787; http://dx.doi.org/10.1093/hmg/ddp347.
40. Kim JM, Hong K, Lee JH, Lee S, Chang N. Effect of folate deficiency on placental DNA methylation in hyperhomocysteinemic rats. J Nutr Biochem 2009; 20:172-6; PMID:18547797; http://dx.doi.org/10.1016/j.jnutbio.2008.01.010.
41. Livak KJ, Schmittgen TD. Analysis of relative gene expression data using real-time quantitative PCR and the 2(-Delta Delta C(T)) Method. Methods 2001; 25:402-8; PMID:11846609; http://dx.doi.org/10.1006/meth.2001.1262.
42. Shen LL, Guo Y, Chen XL, Ahmed S, Issa JPJ. Optimizing annealing temperature overcomes bias in bisulfite PCR methylation analysis. Biotechniques 2007; 42:48, 50, 52 passim; PMID:17269485; http://dx.doi.org/10.2144/000112312.
43. Reed K, Poulin ML, Yan L, Parissenti AM. Comparison of bisulfite sequencing PCR with pyrosequencing for measuring differences in DNA methylation. Anal Biochem 2010; 397:96-106; PMID:19835834; http://dx.doi.org/10.1016/j.ab.2009.10.021.